journal

J. Am. Ceram. Soc., 78 [11] 2881–88 (1995)

Synthesis and Properties of $CaAl_2O_4$-Coated Al_2O_3 Microcomposite Powders

Priyadarshi G. Desai* and Zhengkui Xu*

Department of Materials Science and Engineering, University of Illinois at Urbana-Champaign, Urbana, Illinois 61801

Jennifer A. Lewis*

Department of Materials Science and Engineering and the Beckman Institute for Advanced Science and Technology, University of Illinois at Urbana-Champaign, Urbana, Illinois 61801

Novel microcomposite powders, consisting of inert cores (α-Al_2O_3) surrounded by reactive cement-based coatings ($CaAl_2O_4$), were synthesized by a modified Pechini process. The evolution of the crystalline $CaAl_2O_4$ phase during calcination was studied using multiple analytical techniques, including DRIFTS, ^{13}C and ^{27}Al MAS FT-NMR, and XRD, for both pure $CaAl_2O_4$ and $CaAl_2O_4$-coated Al_2O_3 precursor powders. In both powders, decomposition proceeded via hydrocarbon chain scission and removal of ester groups at low temperatures ($T \leq 450$°C), followed by the formation of inorganic carbonates at higher temperatures ($T \geq 450$°C). These decomposition processes were accelerated by the underlying Al_2O_3 cores. Transmission electron microscopy (TEM) of the fully calcined powders showed that the inert α-Al_2O_3 particles were surrounded by relatively uniform $CaAl_2O_4$ coatings ranging in thickness from approximately 10 to 100 nm.

I. Introduction

Calcium aluminate ($CaAl_2O_4$), the principal cementitious phase in calcium aluminate cements (CAC), plays a vital role in the processing and performance of chemically bonded ceramics such as macrodefect-free (MDF) cements.[1] MDF cements are composites typically consisting of unreacted calcium aluminate grains (~65 vol%) embedded in a matrix of poly(vinyl alcohol) and hydration products. While MDF cements have several attractive features such as low-temperature (<100°C) fabrication, high strength and toughness, and good dielectric properties, their inherent moisture sensitivity limits the realization of many potential applications.[2] Previous studies[3–7] have demonstrated that both the polymeric and unreacted cement phases contribute to property degradation in humid environments. To overcome such limitations, we are developing a novel processing approach in which $CaAl_2O_4$-coated inert ceramic (Al_2O_3) particles are substituted for the CAC powder in the starting MDF formulation. The potential advantage of this approach is that one can tailor the resulting MDF microstructure to essentially eliminate the deleterious unreacted cement phase by controlling the coated layer thickness to inert particle size ratio. Our design of these complex powders was inspired by the recent syntheses[8–15] of other coated powders with differing chemistries.

Crystalline $CaAl_2O_4$ has been prepared previously[16–19] by several techniques, including the Pechini process.[20] The Pechini process and its modifications, such as the liquid mix process,[21] are utilized[17,18,20–26] because of the homogeneity achieved at the nanometer scale and the ease with which multication compounds can be synthesized. This process utilizes the ability of hydroxycarboxylic acids (e.g., citric acid) to form chelates with metal ions and to undergo polyesterification when heated with poly hydroxy alcohols such as ethylene glycol. The chemistry of the starting precursor solutions as well as the evolution of intermediate species has been studied in several systems;[22–25] however, this knowledge was lacking for the $CaAl_2O_4$ system. For example, Zhang *et al.*[22] and Tai and Lessing[23] performed rheological measurements on perovskite precursor solutions to understand gel formation during the initial stage of synthesis. Chen and Hu[24] studied the chemistry of $Bi_{1.5}Pb_{0.5}Sr_2Ca_2Cu_3O_x$ precursor solutions using infrared spectroscopy and determined the presence of coordinated complexes between metal ions and carboxylate groups of the citric acid. Finally, Cho *et al.*[25] carried out infrared spectroscopy and thermal analyses to understand the chemistry of titanate resin intermediates during decomposition.

The main objectives of our research were to prepare and study the chemical evolution and properties of $CaAl_2O_4$-coated Al_2O_3 microcomposite powders. A modified Pechini process was developed to synthesize these powders despite the intrinsic low oxide yields. The high viscosity of the precursor system was advantageous in that Al_2O_3 particle mass segregation could be minimized during the coating process. To study the phase evolution of crystalline $CaAl_2O_4$ during microcomposite powder synthesis, we coupled multiple techniques such as ^{13}C and ^{27}Al magic-angle spin (MAS) Fourier transform (FT) nuclear magnetic resonance (NMR) spectroscopy, diffuse reflectance infrared Fourier transform spectroscopy (DRIFTS), and X-ray diffraction (XRD) analyses. To simplify the interpretation of such results, measurements were first carried out on pure $CaAl_2O_4$ powders synthesized in the absence of the Al_2O_3 phase. By comparison, the influence of the Al_2O_3 core particles on the $CaAl_2O_4$ phase evolution during calcination could be determined. Finally, the key properties of the calcined microcomposite powders were characterized, including their morphology, microchemistry, particle size distribution, and specific surface area. Ultimately, our aim is to use these novel cement-coated ceramic particles to fabricate improved chemically bonded ceramics.

II. Experimental Procedure

(1) $CaAl_2O_4$ and $CaAl_2O_4$-coated Al_2O_3 Powder Synthesis

The Ca,Al precursor solutions were prepared using $Ca(NO_3)_2 \cdot 4H_2O$ (Aldrich, Milwaukee, WI) (0.4 mol per mole of citric

M. Grutzeck—contributing editor

Manuscript No. 193170. Received October 3, 1994; approved June 1, 1995.
Supported by the National Science Foundation's Science and Technology Center for Advanced Cement-Based Materials (ACBM) through Grant No. DMR-91-2002.
*Member, American Ceramic Society.

acid), $Al(NO_3)_3 \cdot 9H_2O$ (Aldrich) (0.8 mol per mole of citric acid), ethylene glycol (EM Science, Gibstown, NJ) (2 mol per mole of citric acid), and deionized water (22 mol per mole of citric acid) to facilitate salt dissolution. This procedure was adopted from Ref. 17.

For the synthesis of the microcomposite powders, alumina powder (average particle diameter ≈4.9 μm) (Alcoa A-10, Pittsburgh, PA) was first added to a citric acid/ethylene glycol solution and mixed with deionized water. A well-dispersed suspension was obtained using ultrasonication, with the citric acid serving as a dispersant for the Al_2O_3 particles.[27] An appropriate amount of the aqueous solution of calcium and aluminum nitrate was then added to the Al_2O_3 suspension to yield a final as-calcined powder comprised of 30 vol% $CaAl_2O_4$ and 70 vol% Al_2O_3.

The Ca,Al precursor systems were continuously mixed at approximately 250°C to yield the resin intermediates for pure $CaAl_2O_4$ or $CaAl_2O_4/Al_2O_3$ powders. These intermediate precursor powders, susbsequently referred to as "Ca,Al precursor" for the pure $CaAl_2O_4$ and "Ca,Al precursor-coated Al_2O_3" for the $CaAl_2O_4/Al_2O_3$ powders, were evenly spread (powder bed thickness ≈ 0.1 cm) on a platinum foil (area of 9 × 7 cm^2), and air-calcined in a box furnace to several temperatures between 300° and 900°C at either 1°C/min or 5°C/min. The samples were held at temperature for approximately 5 min, unless otherwise noted. The weight loss for each sample was measured. The carbon content of the calcined powders was analyzed using a Leco (St. Joseph, MI) combustion analyzer (analysis performed by Luvak, Boylston, MA).

(2) *$CaAl_2O_4$ and $CaAl_2O_4$-coated Al_2O_3 Powder Characterization*

The DRIFTS samples were prepared by mixing the partially and as-calcined Ca,Al precursor and Ca,Al precursor-coated Al_2O_3 powders with KBr, using an agate mortar and pestle. The Ca,Al precursor powder-to-KBr weight ratio was 5:95 for the sample calcined at 300°C. This ratio was then adjusted for samples calcined to higher temperatures such that a constant $CaAl_2O_4$:KBr weight ratio was maintained in all DRIFTS samples. This procedure was necessary to account for the associated mass loss at elevated calcination temperatures. The $CaAl_2O_4$:KBr weight ratio was normalized in an analogous way for the Ca,Al precursor-coated Al_2O_3 powders, where the $CaAl_2O_4$ content was held equivalent to that of the pure $CaAl_2O_4$ powders. DRIFTS analysis of these samples was performed using a Nicolet spectrometer (Magna IR 550 spectrometer, Nicolet Instruments, Madison, WI) equipped with a triglycine sulfate (TGS) detector and mounted with a diffuse reflectance cell (COLLECTOR, Spectra-Tech, Shelton, CT) in the optics chamber of the spectrometer. The optics chamber was continuously purged with filtered air, from which $H_2O(g)$ and $CO_2(g)$ were removed. Each spectrum was acquired at a resolution of 2 cm^{-1} and averaged from 128 scans. These spectra were then converted to Kubelka–Munk units.[28] In this form, the observed peak intensities are directly proportional to their respective functional group concentrations within the precursor and final powder samples.[29,30] Thus, the DRIFTS data can be used quantitatively for a given set of samples. A quantitative comparison of DRIFTS spectra between Ca,Al precursor and Ca,Al precursor-coated Al_2O_3 powders calcined at a given temperature is not possible, however, despite the sample preparation approach described above. This difficulty arises due to the surface-sensitive nature of this sampling technique. For a constant $CaAl_2O_4$:KBr weight ratio, the distribution of the precursor phase is preferentially located on the surface of the Ca,Al precursor-coated powders as compared to its bulk distribution in the pure Ca,Al precursor powders, which leads to significant peak intensity differences between these samples.

^{13}C and ^{27}Al MAS FT-NMR spectroscopy was carried out on the partially and fully calcined Ca,Al precursor and Ca,Al precursor-coated Al_2O_3 powders. These spectra were acquired on a multinuclear solids FT-NMR spectrometer (GN 300WB spectrometer, General Electric Medical, Overland, KS), which has a 7.05 T superconducting magnet (^1H frequency = 300 MHz; ^{13}C frequency = 75.44 MHz; ^{27}Al frequency = 78.17 MHz). A total of 5000 scans for ^{13}C NMR and 100 scans for ^{27}Al NMR were signal-averaged for each spectrum. The ^{13}C chemical shifts (δ (ppm)) are reported relative to tetramethyl silane (TMS), with a positive sign corresponding to a less-shielded environment. Samples were spun at 5 kHz at the magic angle (54.7°) in an appropriate probe (Chemagnetics, Fort Collins, CO). The pulse sequence for ^{13}C NMR spectra incorporated a sideband suppression technique, called total suppression of sidebands (TOSS),[31] coupled with cross polarization (CP), using a 2 ms contact time and proton decoupling. TOSS aligns magnetization paths corresponding to different crystallites, thereby causing the centerbands to be in phase and canceling out the sidebands when summed over the powder sample. The cross-polarization technique utilizes the faster relaxation of hydrogen nuclei and thus circumvents the relaxation delay between pulses, otherwise necessary due to the slow relaxation of the ^{13}C nuclei. Hence, this technique preferentially detects proton-containing species. For the ^{27}Al NMR spectra, samples were spun between 4 and 5.4 kHz at the magic angle, and relaxation from a proton decoupled $\pi/2$ pulse was studied. The spectra were obtained at two different rotation speeds to aid in distinguishing the actual peaks from sidebands. ^{27}Al chemical shifts (δ (ppm)) are reported relative to $AlCl_3$ solution, with a positive sign again corresponding to a less-shielded environment. The chemical shift values are reported as peak maxima instead of isotropic peak shifts.

X-ray diffraction (XRD) analysis was carried out on the partially and fully calcined Ca,Al precursor and Ca,Al precursor-coated Al_2O_3 powders to study their crystalline phase evolution as a function of calcination temperature. These measurements were performed using a Rigaku diffractometer (DMax automated powder diffractometer, Rigaku, Danvers, MA) and Cu$K\alpha$ radiation (40 kV, 40 mA). A total of 10 scans were summed for each diffraction pattern obtained.

Transmission electron microscopy (TEM) samples were prepared by dispersing the fully calcined Ca,Al precursor and Ca,Al precursor-coated Al_2O_3 powders in isopropyl alcohol using ultrasonication. A drop of each suspension was deposited on a copper grid covered with a carbon film. These samples were allowed to dry and then carbon-coated. The powders were characterized using a Philips (Mahwah, NJ) 420 microscope with energy-dispersive X-ray analysis (EDAX) capacity at 120 kV.

The particle size distribution and specific surface area of the starting Al_2O_3 powder, and the calcined $CaAl_2O_4$ and $CaAl_2O_4$-coated Al_2O_3 powders were characterized using a sedimentation technique (X-ray Sedigraph Model 5000E, Micromeritics, Norcross, GA) and nitrogen gas adsorption (ASAP 2400, Micromeritics), respectively. A theoretical composite density of 3.65 g/cm^3 was used for the $CaAl_2O_4$-coated Al_2O_3 microcomposite powders in the particle size analysis measurements. This assumes that the $CaAl_2O_4$:Al_2O_3 volumetric ratio is the same for each individual microcomposite particle, and hence, is a source of error if compositional variations are present.

III. Results

(1) *Phase Evolution in Ca,Al Precursor*

The DRIFTS and ^{13}C NMR spectra of the calcined Ca,Al precursor powders are shown in Figs. 1 and 2, respectively. Due to the overlapping peaks in the DRIFTS spectra, a Fourier self-deconvolution routine[32] was used to accurately identify peak positions. The DRIFTS and NMR peak assignments are given in Table I.[33–39] The nitrogen associated with the nitrate-based precursors was eliminated during the continuous mixing step at

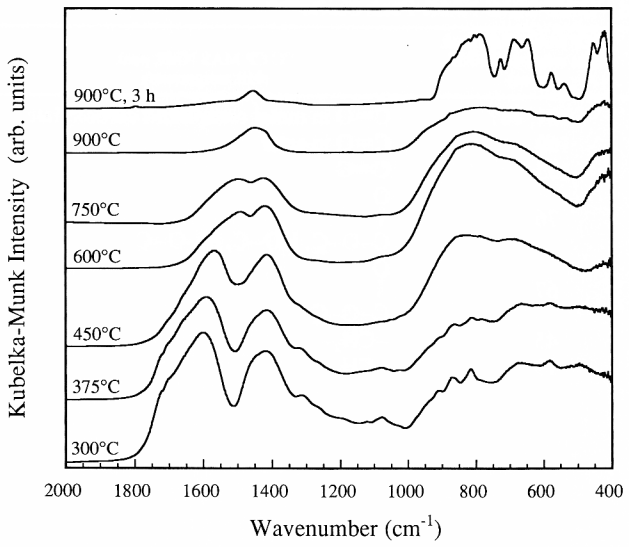

Fig. 1. DRIFTS spectra of Ca,Al precursor powders as a function of calcination temperature (heating rate = 5°C/min).

250°C prior to the formation of the Ca,Al precursor powders, as indicated by elemental analysis.

The NMR peaks at 169 ppm (C=O) and the peaks at 76 and 67 ppm (C—O—C) indicate the presence of ester groups in the Ca,Al precursor powders calcined to 300°C. These groups, corresponding to peaks at 1730 cm^{-1} (C=O) and at 1080 cm^{-1} (C—O), were also detected by DRIFTS analysis. The ester functional groups likely form due to the reaction between the C—OH groups in ethylene glycol and citric acid with the carboxylic acid groups in citric acid. The relative intensity of the ester-related NMR and IR peaks decreases continually for powders calcined between 300° and 450°C, and they can no longer be detected for powders calcined to $T \geq 600$°C. It should be noted that the NMR peak at 76 ppm can also indicate the presence of C—O—H or C—O—M groups. ^{13}C NMR peaks corresponding to unsaturated hydrocarbons (C=C) at approximately 130 ppm with the related DRIFTS peaks at 3062 and 3021 cm^{-1}, and CH_3 groups at 19 ppm with the related DRIFTS peaks at 2969 and 2870 cm^{-1}, were also observed in the Ca,Al precursor powders calcined to 300°C. These functional groups are believed to form as a result of chain scission. There is an attendant reduction of the CH_2 peaks for powders calcined to 375°C as observed by both NMR and DRIFTS. Ultimately, the CH_2 peaks disappear for powders calcined to 450°C, along with a simultaneous increase in the relative intensity of CH_3 and unsaturated hydrocarbon (C=C) peaks.

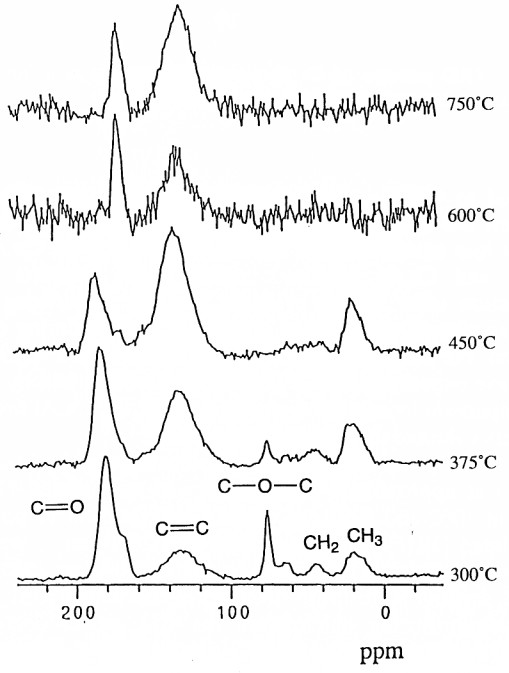

Fig. 2. ^{13}C CP MAS FT-NMR spectra of Ca,Al precursor powders as a function of calcination temperature (heating rate = 5°C/min).

The ^{13}C NMR peaks observed for powders calcined to 600° and 750°C are attributed to metal complexed carboxylates and unsaturated hydrocarbons. Bulk weight loss measurements of the partially calcined Ca,Al precursor powders, shown in Fig. 3, reveal that 93% of the total weight loss occurs by 600°C. This leads to a substantial decrease in the signal-to-noise ratio of the ^{13}C NMR spectra at these temperatures, since the volume fraction of organic species within these powders has been significantly reduced. However, a relatively high amount of carbon (≈9.16 wt%) remains in powders heated to 750°C, as shown in Table II. Two new peaks at 1488 and 1418 cm^{-1} were observed by DRIFTS in the precursor powders calcined to 600° and 750°C, which are assigned to split inorganic carbonate peaks. The splitting of the carbonate peak suggests lower symmetry of the carbonate species present at these temperatures.[39] Upon further calcination to 900°C, the split peaks in the DRIFTS spectra combine to yield a single peak at 1453 cm^{-1}. The intensity of this peak decreases upon continued calcination at 900°C as the concentration of remnant inorganic carbonates decreases. In addition, distinct crystalline $CaAl_2O_4$ peaks emerge in the DRIFTS spectra (between 400 and 820 cm^{-1}) from an earlier broad absorption corresponding to amorphous phases. These crystalline peaks show good agreement with assignments given in Ref. 38 for this phase.

The phase evolution of the Ca,Al precursor powders during calcination was also studied using XRD analysis. Figure 4 shows the XRD patterns for the calcined powders. A significant amount of crystalline $CaAl_2O_4$ can be detected only upon continued calcination at 900°C for 3 h. It should be noted that minor amounts of the $CaAl_4O_7$ phase were observed in the powders calcined to 900°C for 0 h. Both observations are in agreement with previous work by Gulgun *et al.*[17,18]

The local environment of aluminum ions in the partially and fully calcined Ca,Al precursor powders was studied using ^{27}Al NMR spectroscopy to provide information about their bulk coordination. Figure 5 shows ^{27}Al NMR spectra of pure $CaAl_2O_4$ powders as a function of calcination temperature. There was a gradual shift from an octahedral (Al^{VI}) to a tetrahedral (Al^{IV}) coordination with a significant amount of intermediate 5-fold-coordinated species (Al^{V}) observed for powders calcined between 375° and 600°C. Although such significant amounts of pentacoordinated aluminum have not been detected in amorphous aluminum hydroxide gels, they have been previously detected in materials undergoing transformation from octahedral to tetrahedral coordination.[40,41] Upon calcining to 750°C, the Ca,Al precursor powder is still X-ray amorphous (refer to Fig. 4), even though the aluminum ions are mainly tetrahedrally coordinated, as shown in Fig. 5. Using TEM, Gulgun *et al.*[18] have detected microcrystallinity in their Ca,Al precursor powders calcined to 700°C. However, the microcrystalline fraction is very low, which alone cannot explain the predominantly bulk tetrahedral coordination of aluminum in these powders.

(2) Phase Evolution in Ca,Al Precursor-Coated Al_2O_3

The DRIFTS and ^{13}C NMR spectra of the calcined Ca,Al precursor-coated Al_2O_3 powders are shown in Figs. 6 and 7, respectively. Ester groups, corresponding to the ^{13}C NMR peaks at 169, 76, and 67 ppm, and DRIFTS peaks at 1730 and 1080 cm^{-1}, analogous to those present in the Ca,Al precursor powder, were detected in powders calcined to 300°C. The relative intensity of the ester-related ^{13}C NMR and IR peaks decrease for powders calcined to 375°C, and these peaks are no

Table I. Assignment of DRIFTS Peaks and ^{13}C CP MAS NMR Peak Shifts[30–36]

DRIFTS peak positions (cm^{-1})	DRIFTS peak assignments	^{13}C CP MAS NMR peak shifts relative to TMS (ppm)	^{13}C CP MAS NMR peak shift assignments
3062, 3021	CH stretching in alkene	181, 167	C=O in metal complexed carboxylate
2969, 2870	CH stretching in CH_3	169	C=O in ester
2923	CH stretching in CH_2	133	C=C
1730	C=O stretching in COOR	76	O ‖ C–O–C, HO–C, M–O–C
1700	H-bonding of C=O		
1645	Metal carboxylate coordinate complex or OH bending of water	67	O ‖ C–O–C
1600	C=C stretching		
1560–1600	Antisymmetric stretching of metal carboxylates	45	$-CH_2-$
1420, 1450, 1490	Symmetric stretching of metal carboxylates	19	$-CH_3$
1418, 1488	Splitting of C=O stretching in inorganic carbonate		
1450–1465	CH (saturated) bending		
1453	C=O in inorganic carbonate		
1080	C–O stretching (possibly from ester)		
410, 445, 540, 575, 642, 683, 745, 815	$CaAl_2O_4$ peaks		

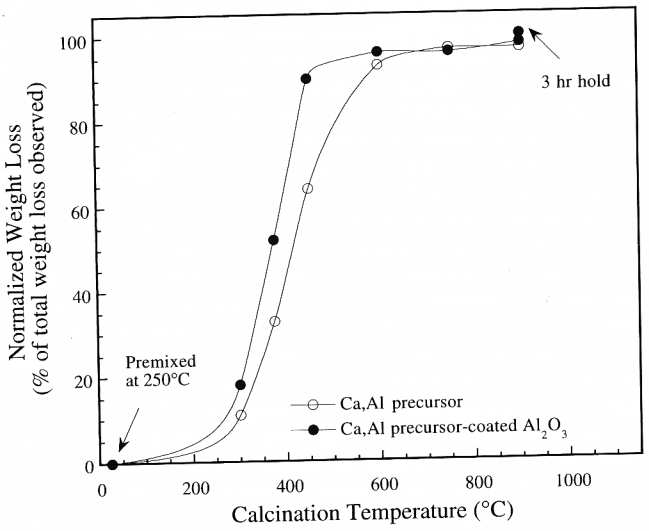

Fig. 3. Normalized weight loss of Ca,Al precursor and Ca,Al precursor-coated Al_2O_3 powders as a function of calcination temperature (heating rate = 5°C/min).

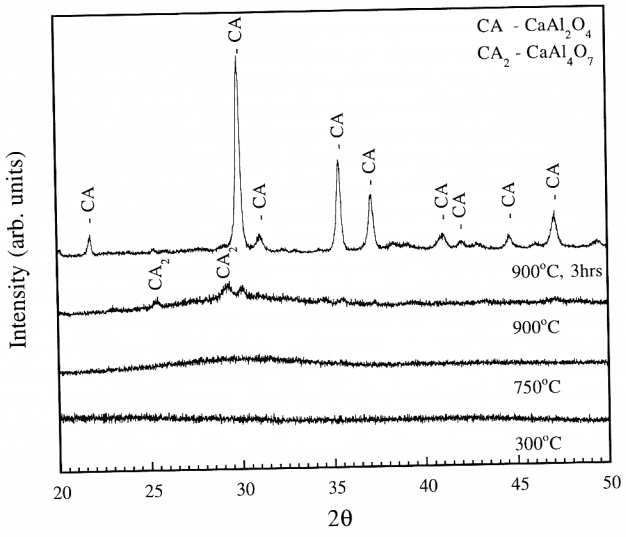

Fig. 4. XRD patterns of Ca,Al precursor powders as a function of calcination temperature (heating rate = 5°C/min).

Table II. Carbon Contents of Powder Samples

Sample	Carbon content (wt%)
Al_2O_3 powder† (as received)	0.03
Ca,Al precursor powder (calcined to)	
750°C	9.16
900°C	1.54
900°C, 3 h	0.36
Ca,Al precursor-coated Al_2O_3 powder (calcined to)	
750°C	1.79
900°C	0.63
900°C, 3 h	0.08

†Alcoa A-10.

longer detected at higher calcination temperatures, $T \geq 450$°C, as shown in Figs. 6 and 7, respectively. The normalized C=O peak intensity (at 1730 cm^{-1}) is plotted as a function of calcination temperature in Fig. 8 for the Ca,Al precursor and Ca,Al precursor-coated Al_2O_3 powders. Clearly, a significant amount of ester groups still remain in the pure Ca,Al precursor powder calcined to 450°C, which suggests that there are differences between the decomposition rates of each powder. The bulk weight loss measurements, shown in Fig. 3, of the Ca,Al precursor and Ca,Al precursor-coated Al_2O_3 powders during calcination offer further evidence that the underlying Al_2O_3 cores accelerate the removal of organic species during decomposition. For example, the Ca,Al precursor-coated Al_2O_3 powders have experienced 90% of their total weight loss by 450°C, in comparison to only 64% weight loss for the Ca,Al precursor powders calcined to the same temperature.

^{13}C NMR peaks corresponding to unsaturated hydrocarbons (C=C) at approximately 130 ppm with the related DRIFTS peaks at 3062 and 3021 cm^{-1}, and CH_3 groups at 19 ppm with the related DRIFTS peaks at 2969 and 2870 cm^{-1}, were also observed in the Ca,Al precursor-coated powders calcined at 300°C, analogous to those detected in the pure Ca,Al precursors. Upon further calcination, the CH_2 peaks decrease at 375°C, disappearing by 450°C, along with a simultaneous increase in the relative intensity of the unsaturated hydrocarbon (C=C) peaks. It should be noted that the ^{13}C NMR spectra of the Ca,Al precursor-coated Al_2O_3 powders calcined to 450°C

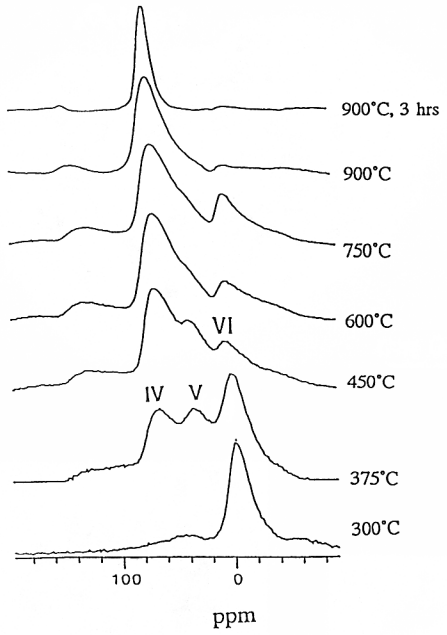

Fig. 5. ^{27}Al MAS FT-NMR spectra of Ca,Al precursor powders as a function of calcination temperature (heating rate = 5°C/min).

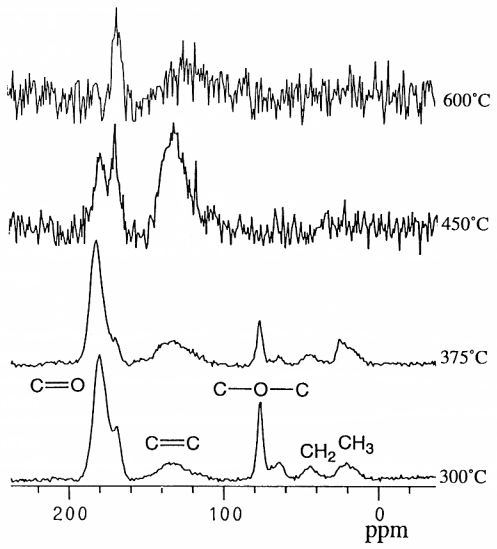

Fig. 7. ^{13}C CP MAS FT-NMR spectra of Ca,Al precursor-coated Al_2O_3 powders as a function of calcination temperature (heating rate = 5°C/min).

exhibited significant deterioration in the signal-to-noise ratio as a result of the accelerated organic decomposition processes.

The Al_2O_3 core particles also influence the development of the intermediate inorganic carbonate phase. Inorganic carbonate peaks at 1488 and 1418 cm^{-1} are detected in significant amounts in the Ca,Al precursor-coated Al_2O_3 powder calcined at 450°C, as shown in the DRIFTS spectra in Fig. 6. In contrast, these peaks were not observed in the Ca,Al precursor powders calcined at this temperature, but emerged only upon heat treatment at higher temperatures ($T \geq 600$°C). XRD analysis of both the Ca,Al precursor and Ca,Al precursor-coated Al_2O_3 powders calcined to several temperatures at a heating rate of 1°C/min in air reveals that the crystalline $CaAl_2O_4$ phase develops earlier in the microcomposite precursor powders, as shown in Fig. 9. For example, strong diffraction peaks corresponding to this phase are observed in the Ca,Al precursor-coated Al_2O_3 powders calcined to 900°C for 0 h. In contrast, these peaks are not observed for the Ca,Al precursor powders calcined under analogous conditions, as discussed previously. The desired phase emerges only upon continued calcination of the pure Ca,Al precursor powders at 900°C.

(3) Properties of $CaAl_2O_4$-coated Al_2O_3 Powder

α-Al_2O_3 and $CaAl_2O_4$ are the two major phases in the microcomposite powders calcined at 900°C for 3 h (refer to Fig. 9). The α-Al_2O_3 phase is detected at all calcination temperatures, solely due to the presence of the underlying α-Al_2O_3 cores. Transmission electron microscopy was used to establish the phase distribution within these powders to ensure that the $CaAl_2O_4$ phase was present in the form of a coating on the α-Al_2O_3 particles, not as separate particles. Figure 10(a) shows the bright-field TEM image of an individual particle representative of the microcomposite powder calcined at 900°C for 3 h, illustrating the presence of a relatively uniform coating approximately 25 nm thick. Fig. 10(b) shows the selected area diffraction (SAD) pattern of this particle. The bright spots are present due to the alumina core, whereas the weak spots accompanied by diffuse streaking originate from the $CaAl_2O_4$ phase. Figure 10(c) shows a dark-field TEM image, taken using a $CaAl_2O_4$ diffraction spot, which clearly demonstrates that the

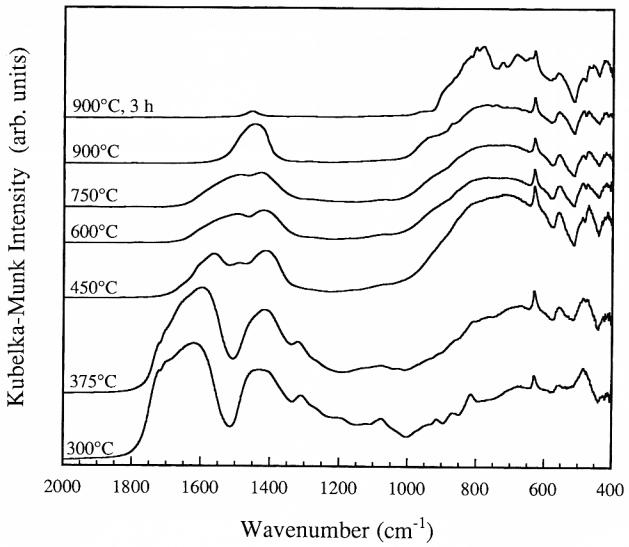

Fig. 6. DRIFTS spectra of Ca,Al precursor-coated Al_2O_3 powders as a function of calcination temperature (heating rate = 5°C/min).

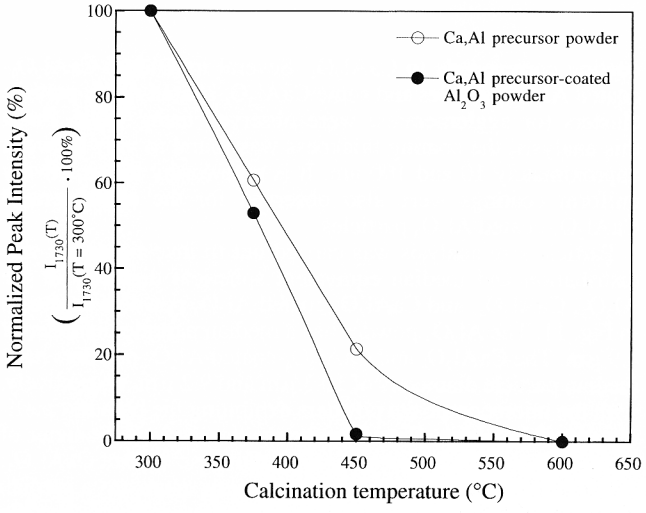

Fig. 8. Normalized DRIFTS peak intensities of ester carbonyl group (1730 cm^{-1}) for Ca,Al precursor and Ca,Al precursor-coated Al_2O_3 powders as a function of calcination temperature (heating rate = 5°C/min).

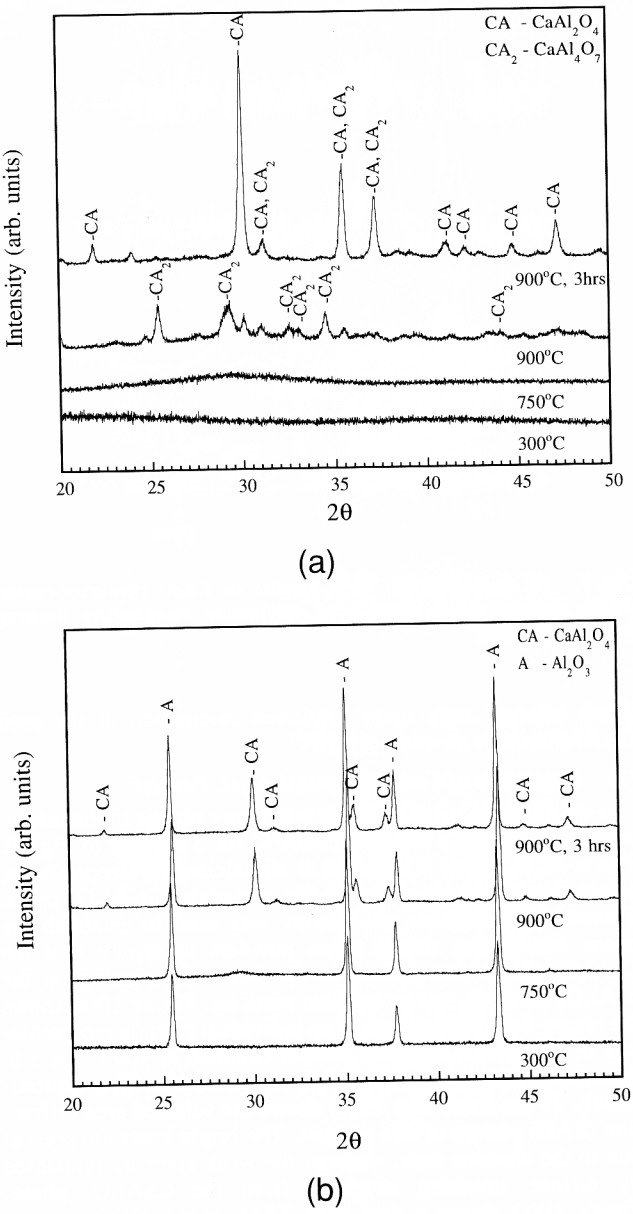

Fig. 9. XRD patterns as a function of calcination temperature for (a) Ca,Al prcursor powders, and (b) Ca,Al precursor-coated Al_2O_3 powders (heating rate = 1°C/min).

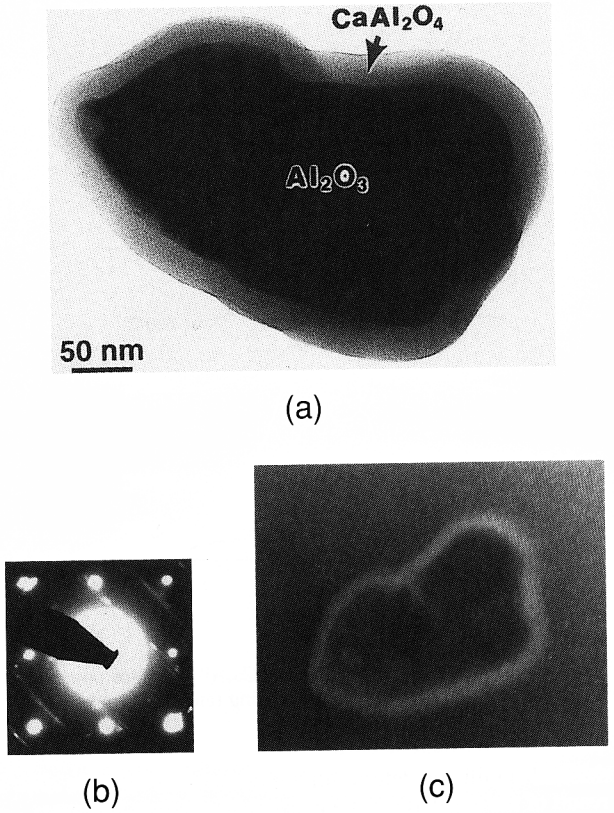

Fig. 10. Electron micrographs of an individual microcomposite $CaAl_2O_4/Al_2O_3$ particle illustrating the uniform $CaAl_2O_4$ coating around an Al_2O_3 particle: (a) bright-field TEM image, (b) SAD spectrum, and (c) dark-field TEM image using a $CaAl_2O_4$ electron diffraction spot.

coating corresponds to $CaAl_2O_4$. Several individual $CaAl_2O_4$-coated Al_2O_3 particles and some $CaAl_2O_4$-coated Al_2O_3 particle clusters (or agglomerates) were observed using TEM. From this analysis, the coating thickness was found to vary between approximately 10 and 100 nm. It is noteworthy that relatively uniform coatings were also observed for the agglomerated $CaAl_2O_4$-coated Al_2O_3 particles.

Particle size analysis was carried out to investigate the size distribution and median equivalent spherical diameter of the Al_2O_3, $CaAl_2O_4$, and $CaAl_2O_4$-coated Al_2O_3 powders as shown in Fig. 11. The Al_2O_3 powder has a median particle diameter of 4.9 μm. The $CaAl_2O_4$ and $CaAl_2O_4$-coated Al_2O_3 powders have median particle diameters of 10.3 μm and 9.2 μm, respectively, with the microcomposite powders exhibiting the broadest particle size distribution. Based on the median particle diameter of the underlying Al_2O_3 cores and the volumetric ratio of $CaAl_2O_4$:Al_2O_3 in the microcomposite powders, one estimates a median diameter of 5.5 μm for these powders, which is lower than the measured value. This difference, combined with the observation of a significant mass fraction of larger particles ($D > 10$ μm) in the microcomposite powders relative to the Al_2O_3 powder, could be attributed to agglomerate formation during the calcination process. In addition, a general broadening of the distribution may also arise from errors associated with assuming a constant theoretical density of 3.65 g/cm^3 for each microcomposite particle. Since TEM analysis reveals variations in coating thicknesses between individual microcomposite particles as well as agglomerated particles which can contain $CaAl_2O_4$-filled internal pores, both of these factors are believed to alter the particle size distribution. Thus, the reported particle size distribution of the $CaAl_2O_4$-coated Al_2O_3 powders can be used only qualitatively to illustrate general trends for this powder.

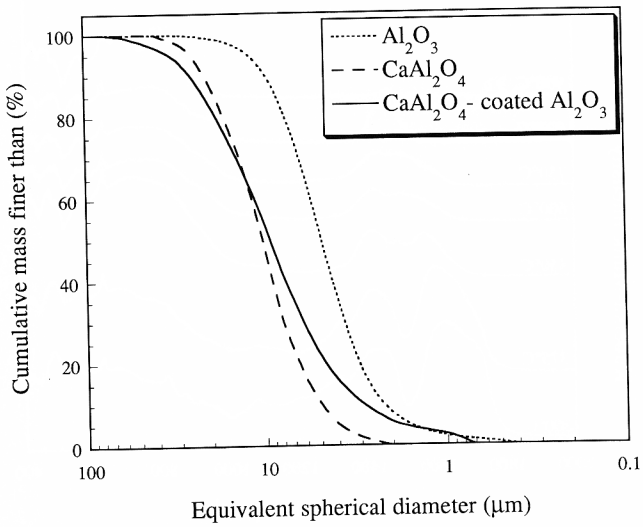

Fig. 11. Cumulative particle size distribution of Al_2O_3, $CaAl_2O_4$, and $CaAl_2O_4$-coated Al_2O_3 powders.

The specific surface areas of the Al_2O_3, $CaAl_2O_4$, and $CaAl_2O_4$-coated Al_2O_3 powders were measured using nitrogen gas adsorption and were found to be 0.75, 3.52, and 3.34 m^2/g, respectively. The large difference in specific surface area between the Al_2O_3 and $CaAl_2O_4$-coated Al_2O_3 powders is not expected, given their respective particle size distributions. Such differences are attributed to the fine-scale intragranular porosity ($D \approx 30$ Å) within the $CaAl_2O_4$ product layer as determined by adsorption–desorption isotherm measurements.

IV. Discussion

Conventional $CaAl_2O_4$ powders are produced by solid-state reactions between calcium carbonate ($CaCO_3$), or calcia (CaO), and Al_2O_3 powders at temperatures above 1400°C.[18] The conventional approach requires not only much higher calcination temperatures than the coated particles, but typically yields final powders with specific surface areas <1 m^2/g and undesirable impurity phases (e.g., $CaAl_4O_7$ and $Ca_{12}Al_{14}O_{33}$). Both of these limitations are overcome by the modified-Pechini approach.

One focus of this study was whether $CaCO_3$ (or CaO) and Al_2O_3 were present as finely distributed intermediate phases prior to the formation of $CaAl_2O_4$ during Ca,Al precursor decomposition. A similar question has been addressed in related investigations carried out on $BaTiO_3$ prepared from solution-derived[42] and Pechini-derived amorphous precursors.[43,44] Recently, Kumar *et al.*[43] have shown that a weakly crystalline, intermediate barium titanium oxycarbonate phase is present prior to the crystallization of $BaTiO_3$ as opposed to crystalline $BaCO_3$ and TiO_2. XRD analysis (refer to Fig. 9) of the partially calcined Ca,Al precursor powders does not reveal the presence of crystalline $CaCO_3$ (or CaO) and Al_2O_3 phases in our samples prior to the formation of $CaAl_2O_4$. DRIFTS analysis of the Ca,Al precursors calcined to 750°C (refer to Fig. 1) indicates the existence of inorganic carbonate functional groups. Furthermore, the bulk of the aluminum ions in these precursors calcined to 750°C are in tetrahedral (Al^{IV}) coordination as determined by ^{27}Al NMR (refer to Fig. 5), as compared to the octahedral(Al^{VI}) coordination expected for Al_2O_3. In previous work,[18] small amounts of nanosized $CaAl_2O_4$ crystallites were observed in powders calcined to similar intermediate temperatures. This observation alone, however, cannot explain the bulk four-fold coordination found in the partially calcined Ca,Al precursor powders. Based on these results, we propose that an intermediate phase other than $CaCO_3$ (or CaO) and Al_2O_3 phases precedes the formation of crystalline $CaAl_2O_4$. One possibility is an amorphous aluminate network consisting of tetrahedrally coordinated aluminate polyhedra $(AlO_4)^-$, where Ca^{2+} ions act as the charge-balancing species.[45–47] In these networks, carbonate species may be discretely located in pockets forming distorted calcium carbonate-like complexes, or may form an integral part of the amorphous structure linking two aluminate polyhedra. Both cases have been previously reported in glasses incorporating such species.[48,49] It should be noted that a large amount of carbon is present in the Ca,Al precursor powders calcined to 750°C (refer to Table II). In future studies, the role of the starting precursor solution chemistry on the carbon content of these intermediate Ca,Al precursor powders will be investigated with the aim of minimizing excess carbon.

A second focus of this study concerned the effects of the Al_2O_3 cores on the decomposition and crystallization of the Ca,Al precursor during calcination. We have clearly shown that organic decomposition processes are enhanced by the presence of the underlying Al_2O_3 cores. This is evident from the DRIFTS (in Figs. 1, 6, and 8), the ^{13}C NMR (in Figs. 2 and 7), and the weight loss measurements (in Fig. 3) as a function of calcination temperature as discussed earlier. Since ceramic surfaces (e.g., Al_2O_3) are well known to catalyze organic decomposition processes[50–52] via extrinsic interactions, these observations are not unexpected. Our results also appear to suggest that the Al_2O_3 cores influence the crystallization kinetics of the $CaAl_2O_4$ phase. XRD analysis of both the Ca,Al precursor and Ca,Al precursor-coated Al_2O_3 powders (refer to Fig. 9) calcined at a heating rate of 1°C/min in air provide evidence of enhanced formation of this phase at 900°C in the latter case. However, Kumar and Messing[44] have recently studied the crystallization kinetics of Pechini-derived Ba,Ti precursor powders and have shown that $BaTiO_3$ formation follows a shrinking core model, whereby the transformation is rate-controlled by the diffusion of $CO_2(g)$ through the nanometer-size intraparticle pores in the product layer. In their work, heat transfer limitations were minimized by choosing an appropriately thin powder bed (bed thickness ≈ 0.1 cm). Their experimental conditions agree well with the bed thickness used during the calcination of the Ca,Al precursor powders, suggesting that heat transfer limitations can also be neglected in the present work. The $CaAl_2O_4$ shell thickness of the calcined Ca,Al precursor-coated Al_2O_3 powders ranged from 10 to 100 nm, which is over two orders of magnitude lower than the average particle size of the calcined Ca,Al precursor powders ($D_{avg} \approx 10.3$ μm). Assuming that the $CaAl_2O_4$ phase formation from the Ca,Al precursor and Ca,Al precursor-coated Al_2O_3 powders also follows the shrinking core model, one could attribute the observed differences in crystallization kinetics between these powders solely to their respective length scale differences. However, it is also conceivable that the underlying Al_2O_3 cores enhance the nucleation of the $CaAl_2O_4$ crystallites. To resolve these effects, additional TEM analysis should be carried out on the partially calcined Ca,Al precursor-coated Al_2O_3 powders.

V. Summary

We have prepared $CaAl_2O_4$-coated Al_2O_3 powders via a modified Pechini process with coating thicknesses between 10 and 100 nm. The chemical evolution of both calcined Ca,Al precursor and Ca,Al precursor-coated Al_2O_3 powders was studied using multiple analytical techniques, which showed that the decomposition process was accelerated by the underlying Al_2O_3 cores. The broad implications of our work are two-fold in nature. First, we have demonstrated that a Pechini-based approach can be readily extended to prepare microcomposite powders coated by complex, multication oxides. For example, one can envision adopting this technique to prepare novel electroceramic powders such as those based on the Pb-La-Zr-Ti-O or Ba-Sr-Ti-O system. Secondly, these reactive $CaAl_2O_4$-coated Al_2O_3 powders are now being utilized to form chemically bonded ceramics (e.g., organocement composites such as MDF cement) at modest processing temperatures ($T \leq 100$°C). Through our synthetic approach, the cement coating thickness and chemical reactivity can be tailored to achieve both the desired final cement content and processibility. As an example, we have recently prepared microcomposite powders with different calcium aluminate cement shell contents of 20 and 30 vol% on varying Al_2O_3 core diameters with mean diameters of 4.9 μm and 0.6 μm, respectively. Further work is needed to define the upper and lower limits of the shell thicknesses that can be reproducibly achieved, the shell thickness distributions, and the core particle sizes which can be effectively coated via this technique, as well as to explore what factors influence the chemical reactivity of this cementitious phase.

Acknowledgments: We would like to thank Mr. D. P. Bentz (at NIST) for proposing the idea of cement-based coated powders, and to Mr. M. A. Gulgun, Mr. M. R. Wegmann, and Professors J. F. Young and A. J. McHugh for useful discussions. We gratefully acknowledge the UIUC Center for Microanalysis of Materials (supported under DEFG02-91-ER45439) for use of their TEM facilities and the UIUC Molecular Spectroscopy Laboratory for use of their NMR facilities.

References

[1]J. D. Birchall, A. J. Howard, and K. Kendall, "Flexural Strength and Porosity of Cements," *Nature (London)*, **289**, 388–89 (1981).

[2]S. R. Tan, A. J. Howard, and J. D. Birchall, "Advanced Materials from Hydraulic Cements," *Philos. Trans. R. Soc. London, A*, **322**, 479–91 (1987).

[3]P. P. Russell, J. Shunkwiler, M. Berg, and J. F. Young, "Moisture Resistance of Macro-Defect-Free Cement"; pp. 501–25 in Ceramic Transactions, Vol. 16,

Advances in Cementitious Materials. Edited by S. Mindess. American Ceramic Society, Westerville, OH, 1991.

[4]J. A. Lewis, M. A. Boyer, and D. P. Bentz, "Binder Distribution in Macro-Defect-Free Cement: Relation between Percolation Properties and Moisture Absorption Kinetics," *J. Am. Ceram. Soc.*, **77** [3] 711–16 (1994).

[5]J. A. Lewis and M. A. Boyer, "The Effects of an Organotitanate Cross-Linking Additive on the Processing and Properties of Macro-Defect-Free Cement," *J. Adv. Cement-Based Mater.*, **2** [1] 2–7 (1995).

[6]N. Kataoka and H. Igarashi, "Expansion Property of Macrodefect-Free Cement in Water"; pp. 195–205 in *Advanced Cements and Chemically Bonded Ceramics*, Proceedings of the MRS International Meeting on Advanced Materials (Sunshine City, Ikeburo, Tokyo, Japan, May 1988). Edited by Masaki Daimon *et al.* Materials Research Society, Pittsburgh, PA, 1989.

[7]P. G. Desai, J. A. Lewis, and D. P. Bentz, "Unreacted Cement Content in Macro-Defect-Free Composites: Impact on Processing-Structure-Property Relations," *J. Mater. Sci.*, **29** [24] 6445–52 (1994).

[8]S. Kratohvil and E. Matijevic, "Preparation and Properties of Coated, Uniform Inorganic Colloidal Particles: 1, Aluminum (Hydrous) Oxide on Hematite, Chromia, and Titania," *Adv. Ceram. Mater.*, **2** [4] 798–803 (1987).

[9]A. K. Garg and L. C. De Jonghe, "Microencapsulation of Silicon Nitride Particles with Yttria and Yttria-Alumina Precursors," *J. Mater. Res.*, **5** [1] 136–42 (1990).

[10]R. E. Partch, Y. Xie, S. T. Oyama, and E. Matijevic, "Preparation and Properties of Uniformly Coated Particles. VIII. Titanium Nitride on Silica," *J. Mater. Res.*, **8** [8] 2014–18 (1993).

[11]B. Djuricic, D. McGarry, and S. Pickering, "The Preparation of Ultrafine Ceria-Stabilized Zirconia Particles Coated with Yttria," *J. Mater. Sci. Lett.*, **12**, 1320–23 (1993).

[12]D. C. Agrawal, R. Raj, and C. Cohen, "In-Situ Measurement of Silica-Gel Coating on Particles of Alumina," *J. Am. Ceram. Soc.*, **72** [7] 2163–64 (1990).

[13]M. D. Sacks, N. Bozkurt, and G. W. Scheiffele, "Fabrication of Mullite and Mullite-Matrix Composites by Transient Viscous Sintering of Composite Powders," *J. Am. Ceram. Soc.*, **74** [10] 2428–37 (1991).

[14]C.-L. Hu and M. N. Rahaman, "Factors Controlling the Sintering of Ceramic Particulate Composites: II, Coated Inclusion Particles," *J. Am. Ceram. Soc.*, **75** [8] 2066–70 (1992).

[15]S. Yang, X. Zhongzi, X. Ping, and T. Mingshu, "A New Method of Enhancing Cement-Aggregate Interfaces, I. Ideal Aggregate and Its Effects on Interfacial Microstructures," *Cem. Concr. Res.*, **22**, 612–20 (1992).

[16]D. M. Roy, R. R. Neurgaonkar, T. P. O'Holleran, and R. Roy, "Preparation of Fine Oxide Powders by Evaporative Decomposition of Solutions," *Am. Ceram. Soc. Bull.*, **56** [11] 1023–24 (1977).

[17]M. A. Gulgun, O. O. Popoola, I. Nettleship, W. M. Kriven, and J. F. Young, "Preparation and Hydration Kinetics of Pure $CaAl_2O_4$"; pp. 199–204 in *Advanced Cementitious Systems: Mechanisms and Properties*, Proceedings of the Materials Research Society Symposium (Boston, MA, December, 1991). Edited by F. P. Glasser *et al.* Materials Research Society, Pittsburgh, PA, 1992.

[18]M. A. Gulgun, O. O. Popoola, and W. M. Kriven, "Chemical Synthesis and Characterization of Calcium Aluminate Powders," *J. Am. Ceram. Soc.*, **77** [2] 531–39 (1994).

[19]B. P. Borglum, "Effect of Processing on Electrical Properties of Calcium Aluminate-Based Chemical Bonded Ceramics"; Ph.D. Thesis. University of Illinois, Urbana-Champaign, IL, 1993.

[20]M. Pechini, "Method of Preparing Lead and Alkaline-Earth Titanates and Niobates and Coating Method Using the Same to Form a Capacitor," U.S. Pat. No. 3 330 697, July 11, 1967.

[21]N. G. Eror and H. U. Anderson, "Polymeric Precursor Synthesis of Ceramic Materials"; pp. 571–77 in *Better Ceramics through Chemistry II*, Proceedings of the Materials Research Society Symposium (Palo Alto, CA, April, 1986). Edited by C. Brinker, D. Clark, and D. Ulrich. Materials Research Society, Pittsburgh, PA, 1986.

[22]S. C. Zhang, G. L. Messing, W. Huebner, and M. M. Coleman, "Synthesis of $YBa_2Cu_3O_{7-x}$ Fibers from an Organic Acid Solution," *J. Mater. Res.*, **5** [9] 1806–12 (1990).

[23]L.-W. Tai and P. A. Lessing, "Modified Resin-Intermediate Processing of Perovskite Powders: Part I: Optimization of Polymeric Precursors," *J. Mater. Res.*, **7** [2] 502–10 (1992).

[24]T.-M. Chen and Y. H. Hu, "Polymeric Precursors for the Preparation of $Bi_{1.5}Pb_{0.5}SR_2Ca_2Cu_3O_x$," *J. Solid State Chem.*, **97**, 124–30 (1992).

[25]S. G. Cho, P. F. Johnson, and R. A. Condrate Sr., "Thermal Decomposition of (Sr,Ti) Organic Precursors during the Pechini Process," *J. Mater. Sci.*, **25**, 4738–44 (1990).

[26]K. D. Budd and D. A. Payne, "Preparation of Strontium Titanate Ceramics and Internal Boundary Layer Capacitors by the Pechini Method"; pp. 239–44 in *Better Ceramics through Chemistry*, Proceedings of the Materials Research Society Symposium (Palo Alto, CA, April, 1984). Edited by C. Brinker *et al.* Materials Research Society, Pittsburgh, PA, 1984.

[27]M. D. Sacks and T. Y. Tseng, "Role of Sodium Citrate in Aqueous Milling of Aluminum Oxide," *J. Am. Ceram. Soc.*, **66** [4] 242–47 (1983).

[28]P. Kubelka, "New Contributions to the Optics of Intensely Light-Scattering Materials, Part I," *J. Opt. Soc. Am.*, **38**, 448–57 (1948).

[29]M. P. Fuller and P. R. Griffiths, "Diffuse Reflectance Measurements by Infrared Fourier Transform Spectrometry," *Anal. Chem.*, **50**, 1906–909 (1978).

[30]P. J. Brimmer and P. R. Griffiths, "Effect of Absorbing Matrices on Diffuse Reflectance Infrared Spectra," *Anal. Chem.*, **58**, 2179–84 (1986).

[31]J. Dixon, "Spinning-Sideband-Free NMR Spectra," *J. Magn. Reson.*, **44**, 220–23 (1981).

[32]J. K. Kauppinen, D. J. Moffatt, H. H. Mantsch, and D. G. Cameron, "Fourier Self-Deconvolution: A Method for Resolving Intrinsically Overlapped Bands," *Appl. Spectrosc.*, **35** [3] 271–76 (1981).

[33]L. J. Bellamy, *The Infrared Spectra of Complex Molecules*, 3rd ed. Chapman and Hall, New York, 1975.

[34]R. A. Nyquist and R. O. Kagel, *Infrared Spectra of Inorganic Compounds*. Academic Press, New York, 1971.

[35]T. M. Duncan, "^{13}C Chemical Shieldings in Solids," *J. Phys. Chem. Ref. Data*, **16** [1] 125–51 (1987).

[36]A. B. Terent'ev, V. I. Dostovalova, and R. Kh. Freidlina, "Carbon-13 NMR Spectra of Branched Carboxylic Acids and Their Derivatives," *Org. Magn. Reson.*, **9**, 301–307 (1977).

[37]A. Samuel-Lewis, P. J. Smith, J. H. Aupers, D. Hampson, and D. C. Povey, "Preparation, Spectroscopic Studies and Structure of Bis(triorganostannyl) Esters of Substituted Aliphatic Dicarboxylic Acids," *J. Organomet. Chem.*, **437**, 131–44 (1992).

[38]J. Bensted, "An Infrared Spectroscopic Examination of High Alumina Cement and Its Hydration Products," *World Cement Technol.*, **13** [2] 85–90 (1982).

[39]F. A. Anderson and L. Brecevik, "Infrared Spectra of Amorphous and Crystalline Calcium Carbonate," *Acta Chem. Scand.*, **45**, 1018–24 (1991).

[40]D. Coster and J. J. Fripiat, "Memory Effects in Gel–Solid Transformations: Coordinately Unsaturated Al Sites in Nanosized Aluminas," *Chem. Mater.*, **5**, 1204–10 (1993).

[41]T. E. Wood, A. R. Siedle, J. R. Hill, R. P. Skarjune, and C. J. Goodbrake, "Hydrolysis of Aluminum—Are All Gels Created Equal?"; pp. 97–116 in *Better Ceramics through Chemistry IV*, Proceedings of the Materials Research Society Symposium (Palo Alto, CA, April, 1990). Edited by C. Brinker *et al.* Materials Research Society, Pittsburgh, PA, 1990.

[42]M. Stockenhuber, H. Mayer, and J. A. Lercher, "Preparation of Barium Titanates from Oxalates," *J. Am. Ceram. Soc.*, **76** [5] 1185–90 (1993).

[43]S. Kumar, G. L. Messing, and W. B. White, "Metal Organic Resin Derived Barium Titanate: I, Formation of Barium Titanium Oxycarbonate Intermediate," *J. Am. Ceram. Soc.*, **76** [3] 617–24 (1993).

[44]S. Kumar and G. L. Messing, "Metal Organic Resin Derived Barium Titanate: II, Kinetics of $BaTiO_3$ Formation," *J. Am. Ceram. Soc.*, **77** [11] 2940–48 (1994).

[45]P. F. Macmillan and B. Piriou, "Raman Spectroscopy of Calcium Aluminate Glasses and Crystals," *J. Non-Cryst. Solids*, **55**, 221–42 (1983).

[46]B. T. Poe, P. F. Macmillan, B. Cote, D. Massiot, and J. P. Coutures, "Magnesium and Calcium Aluminate Liquids: In Situ High Temperature ^{27}Al NMR Spectroscopy," *Science (Washington, D.C.)*, **259**, 786–88 (1993).

[47]J. E. Shelby, C. M. Shaw, and M. S. Spess, "Calcium-Fluoro-Aluminate Glasses," *J. Appl. Phys.*, **66**, 1149–54 (1989).

[48]S. C. Kohn, R. A. Brooker, and R. Dupree, "^{13}C MAS NMR: A Method for Studying CO_2 Speciation in Glasses," *Geochim. Cosmochim. Acta*, **55**, 3879–84 (1991).

[49]J. D. Kubicki and E. M. Stolper, "Structural Roles of CO_2 and $[CO_3]^{2-}$ in Fully Polymerized Sodium Aluminosilicate Melts and Glasses," *Geochim. Cosmochim. Acta*, **59** [4] 683–98 (1995).

[50]H. Knozinger, "Specific Poisoning and Characterization of Catalytically Active Oxide Surfaces"; pp. 184–271 in *Advances in Catalysis*, Vol. 25. Edited by D. D. Eley, H. Pines, and P. B. Weisz. Academic Press, New York, 1976.

[51]M. J. Cima and J. A. Lewis, "Firing-Atmosphere Effects on Char Content from Alumina–Polyvinyl Butyral Films"; pp. 567–74 in Ceramic Transactions, Vol. 1A, *Ceramic Powder Science II*, Proceedings of the First International Conference on Ceramic Powder Processing Science. Edited by G. L. Messing, E. R. Fuller, and H. Hausner. American Ceramic Society, Westerville, OH, 1988.

[52]G. W. Schieffle and M. D. Sacks, "Pyrolysis of Poly(vinyl butyral) Binders: II, Effects of Processing Variables"; see Ref. 51, pp. 559–66. □